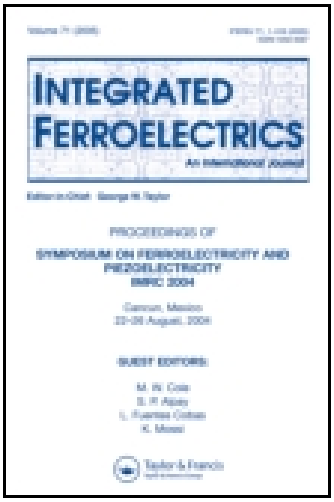

Integrated Ferroelectrics: An International Journal
Publication details, including instructions for authors and subscription information:
http://www.tandfonline.com/loi/ginf20

Enhanced Microwave Absorption Properties of Urchin-like Fe/α-Fe_2O_3 Composite Synthesized by a Simple Thermal Oxidation

Qiangchun Liu[ab], Zhenfa Zi[b], Min Zhang[b], Angbo Pang[a], Jianming Dai[ab] & Yuping Sun[b]

[a] School of Physics and Electronics Information, Huaibei Normal University, Huaibei 235000, People's Republic of China

[b] Key Laboratory of Materials Physics, Institute of Solid State Physics, Chinese Academy of Sciences, Hefei 230031, People's Republic of China

Published online: 09 May 2014.

To cite this article: Qiangchun Liu, Zhenfa Zi, Min Zhang, Angbo Pang, Jianming Dai & Yuping Sun (2014) Enhanced Microwave Absorption Properties of Urchin-like Fe/α-Fe_2O_3 Composite Synthesized by a Simple Thermal Oxidation, Integrated Ferroelectrics: An International Journal, 152:1, 137-143, DOI: 10.1080/10584587.2014.902258

To link to this article: http://dx.doi.org/10.1080/10584587.2014.902258

Integrated Ferroelectrics, 152:137–143, 2014

ISSN: 1058-4587 print / 1607-8489 online
DOI: 10.1080/10584587.2014.902258

Taylor & Francis
Taylor & Francis Group

Enhanced Microwave Absorption Properties of Urchin-like Fe/α-Fe_2O_3 Composite Synthesized by a Simple Thermal Oxidation

QIANGCHUN LIU,[1,2,*] ZHENFA ZI,[2] MIN ZHANG,[2] ANGBO PANG,[1] JIANMING DAI,[1,2,*] AND YUPING SUN[2]

[1]School of Physics and Electronics Information, Huaibei Normal University, Huaibei 235000, People's Republic of China
[2]Key Laboratory of Materials Physics, Institute of Solid State Physics, Chinese Academy of Sciences, Hefei 230031, People's Republic of China

The urchin-like structure of Fe/α-Fe_2O_3 composite has been prepared by a simple thermal oxidation method. The obtained products were characterized by X-ray diffraction (XRD), scanning electron microscopy (SEM) and high-resolution transmission electron microscopy (HRTEM). The microwave absorption property of the Fe/α-Fe_2O_3 composite was measured by vector network analysis (VNA). The excellent microwave absorption property of Fe/α-Fe_2O_3 composite was achieved due to the relatively low permittivity and unique isotropic antenna-like morphology. When the matching thickness is 2.5 mm, the optimal reflection loss of Fe/α-Fe_2O_3 reaches about −41.2 dB at 5.2 GHz. A possible mechanism of the improved microwave absorption properties of the composites was discussed.

Keywords Composite materials; thermal oxidation synthesis; microwave absorption; impedance match

1. Introduction

In recent years, there has been a growing and wide-spread interest in microwave absorption materials due to their military and civil applications such as stealth defense system, microwave interference protection, and microwave darkroom [1–3]. Thus, the development of microwave absorber is strongly demanded [4–6]. Generally, the microwave absorption materials include magnetic loss, dielectric loss, Ohmic loss materials and their mixtures [7–10]. Due to the narrow bandwidth of absorption frequency, single absorber cannot meet the demand of industrial applications. Therefore, the preparation of the composites with excellent microwave absorption performances is a great challenge [11, 12].

Carbonyls iron powders (CIP) have been widely used as microwave absorption materials because of their low cost, large saturation magnetization, and high complex permeability [13]. However, their metallic nature, high permittivity, large eddy-current effects induced by the low resistivity and high oxidation activity of CIP limit severely their applications

Received August 20, 2013; in final form February 7, 2014.
*Corresponding author. E-mail: qchliu@chnu.edu.cn (Q. C. Liu); jmdai@issp.ac.cn (J. M. Dai)
Color versions of one or more of the figures in the article can be found online at www.tandfonline.com/ginf.

[14]. Therefore, surface modification of CIP is necessary to get higher values of complex permeability. Up to date, very early studies [15–18] have reported the formation of micrometer-sized fiber structures by thermally oxidizing iron. Fu et al. [15] have achieved considerable success in the creation of iron oxide nanorods by using a mixture of CO_2, SO_2, and NO_2 gases together with a small amount of H_2O vapor to react with iron at ca. 550°C. Li et al. [16] have obtained urchin-like CIP/α-Fe_2O_3 composite by thermal oxidation at temperatures in the range of 300–450°C. However, up to now, approaches that are simple, direct, controllable, and suitable for large quantity production remain as a challenge for the synthesis of well-crystallized urchin-like structure of FE/α-Fe_2O_3 composite.

In this work, a rapid and simple thermal oxidation method was used to synthesize the urchin-like structure of Fe/α-Fe_2O_3 composite in much higher yields. The morphology, microstructure and microwave absorption performances of the as-prepared samples were also investigated in detail.

2. Experimental

2.1 Materials

Carbonyl Iron powder (CIP) was purchased from Jiangsu Tianyi Co. Ltd. Other reagents used in the experiments were of analytical grade (purchased from Shanghai Chemical Reagent Industrial Company) and used without further purification.

2.2 Synthesis

In a typical synthesis, 10 g CIP and 10 mL ammonia were loaded into a stainless steel autoclave of 50 mL capacity. The autoclave was sealed and put into an electronic furnace; and the temperature of the furnace was increased to 250°C in 50 min and maintained at 250°C for 12 h. Then, the autoclave was cooled to room temperature naturally. It was found that the final products in the autoclave changed to brown powders from gray CIP. The precipitates were dried in a vacuum oven at 60°C for 8 h and collected for characterization.

2.3 Measurements

The phase identification was performed by X-ray diffraction (XRD) on a Bruker Advance D8 X-ray diffractometer with CuKα radiation ($\lambda = 1.5418$Å) in the range from $2\theta = 15^\circ$ to 85° at a scanning rate of 1.5°/min. The morphologies and structures of the synthesized products were observed through a JEOL-6610LV scanning electron microscopy (SEM) and a JEOL JEM-2100 transmission electron microscope (TEM). The complex dielectric permittivity and magnetic permeability were obtained by a vector network analyzer (VNA, AV3629D) using transmission/reflection mode in the frequency range of 1.0–18.0 GHz. The as-prepared composites were mixed uniformly with molten paraffin wax (60 vol.%) and compressed into a cylindrical toroid with an inner diameter of 3.04 mm, an outer diameter of 7.00 mm and a thickness of 2.00 mm. The reflection loss (RL) of samples is simulated by the transmission line theory. The RL of normal incident EM wave at the absorber surface is given by the following equation [19, 20]

$$RL = 20 \log \left| \frac{Z_{in} - Z_0}{Z_{in} + Z_0} \right| \quad (1)$$

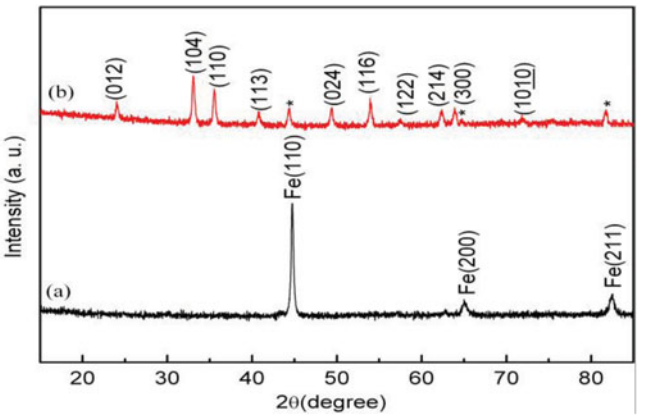

Figure 1. The XRD patterns of CIP (a), Fe/α-Fe_2O_3 composite (b). The positions of the peaks of the CIP are marked with asterisks (*).

Where Z_0 is the impedance of free space, Z_{in} is the input characteristic impedance at the absorber/free space interface, which can be expressed as

$$Z_{in} = Z_0\sqrt{\frac{\mu_r}{\varepsilon_r}}\tanh\left[j\left(\frac{2\pi f t}{c}\right)\sqrt{\mu_r\varepsilon_r}\right] \tag{2}$$

where t is the thickness of the absorber, c is the velocity of the light, f is the frequency, μ_r and ε_r are the relative complex permeability and permittivity, respectively. To evaluate the microwave absorption performances, the RL can be calculated based on Eqs. (1) and (2).

3. Results and Discussion

3.1. Structural Characterization

Fig. 1 shows the XRD patterns of the CIP and as-prepared composites. In Fig. 1(a), the diffraction peaks at $2\theta = 44.85°$, $65.16°$, and $82.34°$ are assigned to (110), (200), (211) planes of α-Fe (JCPDS card No.06-0696), respectively. After thermal oxidation at 250°C for 12 h, the intensity of α-Fe diffraction peaks decreases (in Fig. 1(b)). The peaks at 2θ values of 24.2°, 33.2°, 35.7°, 40.9°, 49.5°, 54.0°, 57.5°,62.4°, 64.0°, 72.0° assign to (012), (104), (110), (113), (024), (116), (122), (214), (300) and (10$\bar{1}$0) planes of the rhomb-centered lattice of α-Fe_2O_3 (JCPDS card No. 86-0550), respectively. No peak of any other phase can be detected except for the peak marked by an asterial referring to the typical Bragg peak for α-Fe. This indicates that α-Fe partly transforms to α-Fe_2O_3 crystals after thermal oxidation at 250°C for 12 h.

A typical SEM image of the CIP is presented in Fig. 2a, which shows that the particles are sphere-like with smooth surfaces and each sphere has a diameter in the range of 0.5-3μm. Figs. 2b and 2c show the typical SEM images of Fe/α-Fe_2O_3 composites, which were synthesized at 250°C for 12 h by the simple thermal oxidation. From Figs. 2b and 2c, we can see urchin-like Fe/α-Fe_2O_3 composites formed with tip diameters ranging from 10–20 nm and lengths of a few mm. The high-resolution TEM (HR-TEM) observation found that the nanoflake has a single-crystal structure with the [110] growth direction along its long axis. The d-spacing of 0.251 nm reveals that the nanoflake is single-crystal α-Fe_2O_3.

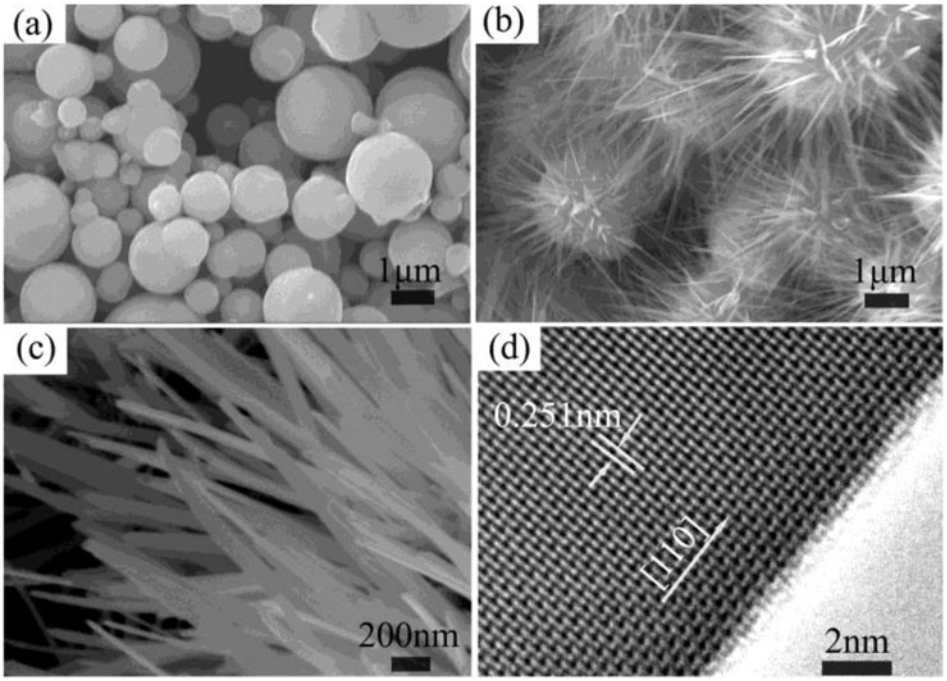

Figure 2. SEM images of CIP (a), Fe/α-Fe_2O_3 composite (b,c), and HRTEM of α-Fe_2O_3 (d).

3.2 Microwave Absorption Properties

Fig. 3a shows real part (ε') and imaginary part (ε'') of the relative complex permittivity of the CIP and Fe/α-Fe_2O_3 composite in the frequency range of 1.0–18.0 GHz. Both ε' and ε'' values of CIP are as large as 54.0 and 11.8 at 1.0 GHz, respectively, and then decrease in the higher frequency range. After coating a layer of α-Fe_2O_3 crystals, the permittivity of Fe/α-Fe_2O_3 composite substantially decreases and almost keeps constant in the whole frequency range. The value of ε' at 1.0 GHz is about 29.0 and the value of ε'' is about 10.7, respectively. According to the free electron theory [21], $\varepsilon'' = 1/\rho\omega\varepsilon_0$, where ω, ε_0 and ρ are the angular frequency, the dielectric constant of free space and the resistivity, respectively, it can be speculated that CIP has lower electric resistivity than α-Fe_2O_3 due to the metallic behavior of CIP. In general, the real part of permittivity is mainly related to the polarization, and the imaginary part implies the dielectric loss in the metal particles [22]. In the metal-based composites, two kinds of mechanisms for the polarization were reported: space charge polarization and dipole polarization. The presence of Fe_2O_3 crystals with higher electric resistivity on the surfaces of CIP can prevent the formation of electric conducting networks and decrease the space charge polarization. Consequently, the weaker space charge polarization and higher electric resistivity result in the relatively low permittivity of Fe/α-Fe_2O_3 composite.

Fig. 3b shows real part (μ') and imaginary part (μ'') of the complex magnetic permeability of the CIP and Fe/α-Fe_2O_3 composite. The μ' values of CIP exhibit a sharp decrease in the 1.0–6.0 GHz from 5.4 to 2.2 and retain a gradual decrease over 6.0–18.0 GHz. The μ'' curve of CIP exhibits a peak at 2.1 GHz, which attributes to natural resonance of CIP. And then, the μ'' values decrease abruptly from 2.2 to 0.5 in the range of high

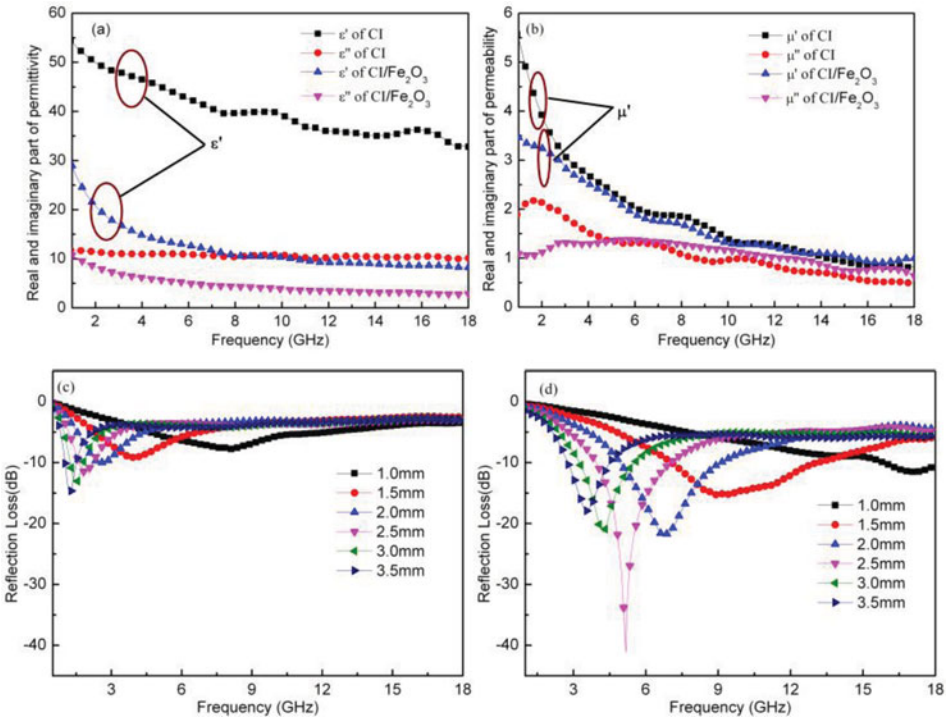

Figure 3. The frequency dependence real part ε', imaginary part ε'' of complex permittivity (a), real part μ' and imaginary part μ'' of complex permeability (b), reflection loss with different thicknesses of CIP (c), Fe/α-Fe$_2$O$_3$ composite (d).

frequency due to the effect of eddy currents at high frequency. The low μ'' values limit the application especially at high frequency. Compared with CIP, the μ' and μ'' values, after coating a layer of α-Fe$_2$O$_3$ crystals, are lower in the range of low frequency and higher in the range of high frequency. Meanwhile, the frequency of natural resonance shifts to high frequency from 2.1 to 2.8 GHz after coating a layer of α-Fe$_2$O$_3$ crystals. The shift of natural resonance may be ascribed two following reasons. On the one hand, the saturation magnetizations of the as-synthesized Fe/α-Fe$_2$O$_3$ composites are smaller than that of CIP because of the nonmagnetic α-Fe$_2$O$_3$. On the other hand, mixing Fe/α-Fe$_2$O$_3$ with paraffin wax causes the decrease of saturation magnetization of the composites. According to Kittel equation [23]: $f_\gamma = \gamma H_a$, where f_γ is the resonance frequency, γ is the gyromagnetic ratio and $H_a = 4\,|K_1|\,/3\mu_0 M_s$, we can deduce that the natural resonance peak will shift to high frequency with the decreased M_s. From Fig. 3b, we also can see that the μ' and μ'' values of the Fe/α-Fe$_2$O$_3$ composites prepared in this work is also higher than that of ferromagnetic alloy-oxide composites reported elsewhere. For example, the μ' and μ'' values with 75 wt.% flower-like ZnO/carbonyl-iron composites as fillers prepared by Ma et al. [24] decreases from around 1.9 to 0.9 and around 0–0.5 in the range of 2–18 GHz, respectively. The μ' of composites with 29 vol.% Fe microwires as fillers prepared by Liu et al. [25] decreases from 1.8 to 0.9. The μ' and μ'' values are comparable to 30 vol.% planar anisotropy carbonyl-iron particles [26]. Additionally, a multi-resonance behavior can also be observed for the Fe/α-Fe$_2$O$_3$ composite, which is ascribed to the inhomogeneous particle sizes or"super-exchange mode" resonance created between the Fe/α-Fe$_2$O$_3$.

The reflection loss (RL) values of the CIP and Fe/α-Fe_2O_3 composite as a function of frequency are shown in Figs. 3c and 3d. It is clearly found that the minimum RL of two samples moves toward lower frequency band with the increasing thickness from 1.0 to 3.5 mm. The RL value for CIP (Fig. 3c) less than -10 dB is obtained in the 1.2–2.5 GHz with absorber thickness of 2.0–3.5 mm. In contrast, the minimum RL value for the urchin-like Fe/α-Fe_2O_3 composite is –41.2 dB (more than 99.9% of EM wave absorption) at 5.2 GHz (C band). The effective absorption bandwidth exceeding -20 dB reaches 0.8 GHz (from 4.8 to 5.6 GHz). RL values of less than –10 dB were observed in the range of 3.6–17.2 GHz with absorber thickness of 1.0–3.5 mm. Compared with ZnO-coated Fe nanocapsules [27] and Ni/C nanocapsules [21] reported in previous literatures, the urchin-like Fe/α-Fe_2O_3 composite apparently has excellent absorption properties. The results indicate that the α-Fe_2O_3 crystal has an obvious effect on the reflection loss of composites. As we know, the design of microwave absorption materials with low reflection requires two important conditions: impedance matching characteristic and attenuation characteristic. To obtain low reflection, impedance matching has to be satisfied, i.e., μ^* equals ε^*, where $\mu^* = \mu'$-jμ'' and $\varepsilon^* = \varepsilon'$-j$\varepsilon''$. But for most of the magnetic materials, μ' is less than ε' at high frequency. Therefore, higher values of μ' and μ'' and appropriate values of ε' and ε' are required. As to the CIP, the ε' and ε'' values are so large that it is difficult to attain impedance match, which means most of the incident microwave reflects from the surface of CIP. Hence, the microwave absorption property of CIP is unsatisfactory. After coating a layer of α-Fe_2O_3, the ε' and ε'' values decrease and the μ' and μ'' values remain relatively high, which leads to the easier penetration and absorption of incident microwave. On the other hand, the urchin-like structure of Fe/α-Fe_2O_3 composite with the unique isotropic antenna-like morphology attributes to the excellent absorption properties. Therefore, the absorption properties of the urchin-like Fe /α-Fe_2O_3 composite will be enhanced.

4. Conclusion

The urchin-like structure of Fe/α-Fe_2O_3 composite has been prepared by a simple thermal oxidation method. The as-prepared Fe/α-Fe_2O_3 composite shows excellent electromagnetic absorption properties. It has an optimal RL of about –41.2 dB at 5.2 GHz with 2.5 mm thickness layer. The effective absorption bandwidth exceeding -20 dB reaches 0.8 GHz (from 4.8 to 5.6 GHz). Therefore, the optimal RL and the broad bandwidth of RL qualify urchin-like Fe/α-Fe_2O_3 composite to be a prominent candidate for microwave absorption applications.

Funding

This work was financially supported by the National Nature Science Foundation of China (51002156, 11274314 and 11104098).

References

1. H. M. Musal, and H. T. Hahn, Thin-layer electromagnetic absorber design. *IEEE Trans. Magn.* **25**, 3851–3853 (1989).
2. J. Y. Shin, and J. H. Oh, the microwave absorbing phenomena of ferrite microwave absorbers. *IEEE Trans. Magn.* **29**, 3437–3439 (1993).
3. S. Sugimoto, T. Maeda, D. Book, T. Kagotani, K. Inomata, M. Homma, H. Ota, Y. Houjou, and R. Sato, *J. Alloys Compd.* **330**, 301–306 (2002).

4. Q. Liu, Z. Zi, D. Wu, Y. Sun, and J. Dai, Controllable synthesis and morphology-dependent microwave absorption properties of iron nanocrystals. *J. Mater. Sci.* **47**, 1033–1037 (2012).
5. R. C. Che, C. Y. Zhi, C. Y. Liang, and X. G. Zhou, *Appl. Phys. Lett.* **88**, 033105 (2006).
6. P. Toneguzzo, G. Viau, O. Acher, F. Fievet-Vincent, and F. Fievet, *Adv. Mater.* **10**, 1032–1035 (1998).
7. G. Sun, B. Dong, M. Cao, B. Wei, and C. Hu, Hierarchical Dendrite-Like Magnetic Materials of Fe_3O_4, γ-Fe_2O_3, and Fe with High Performance of Microwave Absorption. *Chem. Mater.* **23**, 1587–1593 (2011).
8. F. Xia, J. Liu, D. Gu, P. Zhao, J. Zhang, and R. Che, Microwave absorption enhancement and electron microscopy characterization of $BaTiO_3$ nano-torus. *Nanoscale* **3**, 3860–3867 (2011)
9. H. L. Zhu, Y. J. Bai, R. Liu, N. Lun, Y. X. Qi, and F. D. Han, *et al.*, In situ synthesis of one-dimensional MWCNT/SiC porous nanocomposites with excellent microwave absorption properties. *J. Mater. Chem.* **21**, 13581–13587 (2011).
10. C. L. Zhu, M. L. Zhang, Y. J. Qiao, G. Xiao, F. Zhang, and Y. J. Chen, Fe_3O_4/TiO_2 Core/Shell Nanotubes: Synthesis and Magnetic and Electromagnetic Wave Absorption Characteristics. *J. Phys. Chem. C* **114**, 16229–16235 (2010).
11. F. Tabatabaie, M. H. Fathi, A. Saatchi, and A. Ghasemi, Microwave absorption properties of Mn- and Ti-doped strontium hexaferrite. *J. Alloys Compd.* **470**, 332–335 (2009).
12. A. Katsounaros, K. Z. Rajab, Y. Hao, M. Mann, and W. I. Milne, Microwave characterization of vertically aligned multiwalled carbon nanotube arrays. *Appl. Phys. Lett.* **98**, 203105 (2011).
13. R. B Yang, C. Y Tsay, D. S. Hung, W. F. Liang, Y. D. Yao, and C. K. Lin, Complex permittivity and permeability of iron-based composite absorbers measured by cavity perturbation method in X-band frequency range. *J. Appl. Phys.* **105**, 07A528 (2009).
14. M. Han, W. Tang, W. Chen, H. Zhou, and L. Deng, Effect of shape of Fe particles on their electromagnetic properties within 1–18 GHz range. *J. Appl. Phys.* **107**, 09A958 (2010).
15. Y. Y. Fu, R. M. Wang, J. Xu, J. Chen, Y. Yan, A. V. Narlikar, and H. Zhang, Synthesis of large arrays of aligned α-Fe_2O_3 nanowires. *Chem. Phys. Lett.* **379**, 373–379 (2003).
16. H. C. Yu, L. C. Hsu, T. H. Chang, and Y. Y. Li, A 3D α-Fe_2O_3 nanoflake urchin-like structure for electromagnetic wave absorption. *Dalton Trans.* **41**, 723–726 (2012)
17. G. X. Tong, J. H. Yuan, J. Ma, J. G. Guan, W. H. Wu, L. C. Li, and R. Qiao, Polymorphous Fe/Fe_xO_y composites: One-step oxidation preparation, composition control, and static magnetic and electromagnetic characteristics. *Mater. Chem. Phys.* **129**, 1189–1194 (2011).
18. L. C. Hsu, and Y. Y. Li, Direct electrical measurement of an individual α- Fe_2O_3 nanobridge field effect transistor formed via one-step thermal oxidation. *Appl. Phys. Lett.* **93**, 083113 (2008).
19. P. A. Miles, W. B. Westphal, and A. Vonhippel, Dielectric spectroscopy of ferromagnetic semiconductors. *Rev. Mod. Phys.* **29**, 279–307 (1957).
20. E. Michielssen, J. M. Sajer, S. Ranjithan, and R. Mittra, Design of lightweight, broad-band microwave absorbers using genetic algorithms. *IEEE Trans.Microwave Theor. Tech.* **41**, 1024–1031 (1993).
21. X. F. Zhang, X. L. Dong, H. Huang, Y. Y. Liu, W. N. Wang, and XG Zhu, *et al.*, Microwave absorption properties of the carbon-coated nickel nanocapsules. *Appl. Phys. Lett.* **89**, 053115 (2006)
22. Z. Han, D. Li, X. Liu, D. Geng, J. Li, and Z. Zhang, Microwave-absorption properties of Fe(Mn)/ferrite nanocapsules. *J. Phys. D: Appl. Phys.* **42**, 055008 (2009).
23. C. Kittel, On the theory of ferromagnetic resonance absorption. *Phys. Rev.* **73**, 155–161 (1948).
24. Z. Ma, Y. Zhang, C. Cao, J. Yuan, Q. Liu, and J. Wang, Attractive microwave absorption and the impedance match effect in zinc oxide and carbonyl iron composite. *Phys. Rev. B: Condens. Matter* **406**, 4620–4624 (2011).
25. J. Liu, M. Itoh, M. Terada, T. Horikawa, and K. Machida, Enhanced electromagnetic wave absorption properties of Fe nanowires in gigaherz range. *Appl. Phys. Lett.* **91**, 093101 (2007).
26. R. Han, L. Qiao, T. Wang, and F. Li, Microwave complex permeability of planar anisotropy carbonyl-iron particles. *J. Alloys Compd.* **509**, 2734–2737 (2011).
27. X. G. Liu, D. Y. Geng, H. Meng, P. J. Shang, and Z. D. Zhang, Microwave-absorption properties of ZnO-coated iron nanocapsules. *Appl. Phys. Lett.* **93**, 173117 (2008).